Faculty Publications   Physics and Astronomy, Department of

7-27-1981

Macroscopic Quantum Tunneling in 1-μm Nb Josephson Junctions

Richard F. Voss

Richard A. Webb
University of South Carolina - Columbia, webbra@mailbox.sc.edu

Follow this and additional works at: https://scholarcommons.sc.edu/phys_facpub

Part of the Physics Commons

Macroscopic Quantum Tunneling in 1-μm Nb Josephson Junctions

Richard F. Voss and Richard A. Webb

IBM Thomas J. Watson Research Center, Yorktown Heights, New York 10598

(Received 24 April 1981)

The probability distributions for switching out of the superconducting state of low-current-density 1-μm Nb Josephson junctions with capacitance ≈ 0.1 pF have been measured as a function of temperature T down to 3 mK. Below 100 mK the distribution widths become independent of T. The results are in excellent agreement with predictions for the quantum tunneling of the (macroscopic) junction phase that include the reduction of tunneling rates due to dissipation.

At high temperatures a macroscopic system in a metastable state undergoes transitions to a lower energy state via thermal excitation over the intervening barrier. At sufficiently low T, however, transitions can only occur via a quantum mechanical tunneling through the barrier. This latter process, known as macroscopic quantum tunneling (MQT), is of great theoretical and experimental interest.[1-9] Both Josephson junctions and superconducting loops containing a junction have been proposed as possible experimental systems for the study of these transitions. Unlike microscopic tunneling, MQT involves the collective behavior of many degrees of freedom and macroscopic dissipation is expected to play an important role.[3-5] Although recent experiments on superconducting loops (rf SQUID's) have been interpreted in terms of MQT,[7,8] such interpretations are doubtful. Not only are the measurements rather indirect, but the Josephson elements (point contacts) are not well characterized and the effects require much higher tunneling rates than expected for a reasonable choice of junction parameters. On the other hand, preliminary measurements on high-current-density junctions[9] from 1.5 to 4.2 K show temperature-dependent rates smaller than expected from a simple WKB calculation. In this Letter, we show that careful measurements on well characterized low-current-density Josephson junctions down to 3 mK give tunneling rates in excellent agreement with theoretical predictions[3,4] that include a reduction due to dissipation.

The classical equation of motion of a Josephson junction of critical current I_c (supercurrent $I_0 \sin\theta$ where θ is the phase difference across the junction) shunted by a resistance R and capacitance C and driven by an external constant current I can be written in the form

$$C\ddot{s} + \frac{\dot{s}}{R} + \frac{\partial U(s)}{\partial s} = 0. \tag{1}$$

The junction voltage $V = \varphi_0 \dot{\theta}/2\pi = \dot{s}$, where φ_0 is the flux quantum. This formulation corresponds to the motion of a particle of mass C in the one-dimensional potential

$$U(s) = \frac{I_c \varphi_0}{2\pi}\left[\frac{2\pi s x}{\varphi_0} + \cos\left(\frac{2\pi s}{\varphi_0}\right)\right].$$

For $x = I/I_c < 1$, $U(s)$ consists of a series of wells separated by barriers of height

$$H(x) = (I_c \varphi_0/\pi)[(1-x^2)^{1/2} - x\cos^{-1}x] - \hbar\omega_0/2,$$

which is reduced by the zero-point energy $\hbar\omega_0/2$. The natural frequency of the particle in the well, ω_0, is related to the Josephson frequency ω_J $= (2\pi I_c/\varphi_0 C)^{1/2}$ of the junction by $\omega_0 = \omega_J(1-x^2)^{1/4}$. Confinement in a single well corresponds to the superconducting state of the junction. For $\beta_c = (\omega_J R C)^2 = 2\pi I_c R^2 C/\varphi_0 \gtrsim 1$, the motion is underdamped and a transition out of the well leads to continuous motion of the particle down the potential and a switching to the finite voltage state in the junction.

At high temperatures the transition rate out of the metastable state is dominated by thermal activation over the barrier $H(x)$. The thermal rate,

$$\tau_{th}^{-1} = (\omega_0/2\pi)\exp[-H(x)/k_B T], \tag{2}$$

has been well verified[10] for junctions above 1.5 K. As $T \to 0$ the transition rate is dominated by the quantum mechanical tunneling of the macroscopic junction phase. Path integral techniques[3,4] can be used to calculate the tunneling rate and the result can be cast in the form

$$\tau_{MQT}^{-1} = \frac{\omega_0}{2\pi}\left(\frac{b}{2\pi}\right)^{1/2} e^{-b}, \tag{3}$$

where

$$b = \frac{\alpha H(x)}{\hbar\omega_0} + \frac{A(\Delta s)^2}{\hbar R}. \tag{4}$$

The first term in Eq. (4) is the usual tunneling exponent (in a form similar to the WKB calculation[2] for the superconducting ring) while α is a factor depending on the shape of the barrier (α = 7.2 for a cubic potential appropriate to a junction[4] with I near I_c). The second term represents the lowest-order dissipative corrections, where A is a numerical factor of order unity and Δs is the distance under the barrier. Near its maximum $U(s) \approx H(x) - \omega_0^2 C s^2/2$, $(\Delta s)^2 \approx 8H(x)/\omega_0^2 C$, and

$$b \approx (7.2 + 8A/\omega_0 RC)H(x)/\hbar\omega_0. \qquad (5)$$

In the absence of dissipation, we expect a transition from thermal activation to tunneling when $k_B T \approx \hbar\omega_0/7$. In the above formulation dissipation reduces the crossover temperature. Although increases with dissipation have also been predicted,[5] Eqs. (3) and (5) provide a convenient framework for comparison with experiment.

The junctions used in the experiment were patterned on Si chips with use of electron beam lithography in a crossed strip geometry with an overlap area of $1\,\mu m$.[2] Both base and counter electrodes were made of electron beam evaporated Nb with $T_c \approx 9$ K. An rf plasma discharge was used to grow the oxide tunnel barrier. Similar junctions have been extensively studied for dc SQUID's and other applications.[11] The capacitance of the junctions is estimated both from dc SQUID resonances[12] and oxide studies[13] to be 0.1 ± 0.2 pF. The junctions had a uniform critical current density as evidenced by the fact that I_c could be modulated to near zero with a magnetic field.

The samples were placed inside the copper mixing chamber of a dilution refrigerator to ensure maximum thermal coupling. A low-frequency sinusoidal current (amplitude $\approx 2I_c$) was applied to the junction and the distribution of currents at which the junction switched out of the superconducting state was measured. Extensive efforts were made to isolate the sample from external noise. Connections to room-temperature electronics were made through cooled 2-kΩ resistors. The large cable capacitance together with the 2-kΩ resistors and large sample impedance gave electrical cutoff frequencies $\lesssim 1$ kHz. The computerized measurement apparatus was located outside the screened room that contained the refrigerator and a series of isolation amplifiers and filters. The low current densities and slow (10–20 Hz) current sweeps ensured that the junctions were at the bath temperature in the superconducting state with no dissipation prior to

switching. In fact, measurements using the same apparatus on other samples (two-dimensional arrays of 20 000 1-μm Nb junctions) of comparable impedance and I_c on the same chip showed temperature-dependent effects well below 20 mK.

Typical distributions consisted of 200 000 events measured over about five hours at constant temperature. Figure 1 shows a series of switching probability distributions $P(I)$ versus applied current I at various T for a junction with a maximum $I_c \approx 1.6$ μA. As T is lowered $P(I)$ narrows and moves to higher I. All $P(I)$ have a characteristic asymmetry with a tail at low I and a more abrupt cutoff at high I as expected from theory. With the measurement of the complete $P(I)$ we could ensure that neither low-frequency noise [which would smear out $P(I)$ to approach a Gaussian distribution] nor external transients [$P(I)$ independent of I at low I] influenced the switching.

The inset shows the highly hysteretic ($\beta_c \approx 50$) I-V characteristic of the sample at 95 mK. As is common in all-Nb junctions, the samples had a significant normal conductance, similar to an external shunt, in parallel with the usual tunneling currents. Although undesirable for many digital applications, this temperature-independent (below 2 K) conductance provided a well-defined R [appropriate for Eq. (1)] that we shall use for comparison with theory.

The measured $P(I)$ can be related[10] to the transition rate $\tau^{-1}(I)$ by

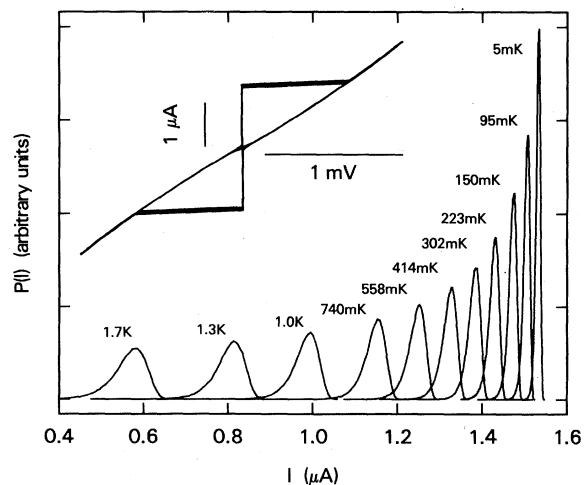$$P(I) = \tau^{-1}(I)\,|\,dI/dt|^{-1}[\,1 - \int_0^I P(i)\,di\,].$$

FIG. 1. Switching distribution $P(I)$ vs I out of the superconducting state for a 1-μm Nb junction at various T. Inset shows four traces of the I-V charactistic at 95 mK.

Figure 2(a) shows $\tau^{-1}(I)$ calculated from the measured $P(I)$ of the junction in Fig. 1. Figure 2(b) shows $\tau^{-1}(I)$ calculated from the $P(I)$ for a junction with an order of magnitude smaller I_c and smaller damping ($\beta_c \approx 5000$). In both cases, $\ln\tau^{-1}(I)$ is roughly proportional to I. As T decreases $\tau^{-1}(I)$ moves to higher I and the slope of $\ln\tau^{-1}(I)$ increases. For $T \lesssim 100$ mK there is little change in either the slope shown in Fig. 2 or the width of $P(I)$. I_c, however, continues to increase slightly as T is lowered.

The I_c of each junction is estimated by fitting the high-T $\tau^{-1}(I)$ to Eq. (2). Such fits are very sensitive to small changes in I_c and are accurate to within 5%. For the high-I_c junction we find $I_c = 1.62$ μA and for the low-I_c junction $I_c = 162$ nA. These fits are shown as the solid lines marked "thermal" in Fig. 2. Since the Nb $T_c \approx 9$ K and the measured R was independent of T for $T \lesssim 2$ K, we believe that I_c is also independent of T in this range.

Using the above values of I_c with $C = 0.1$ pF we can estimate the tunneling rates from Eq. (3). The estimates without dissipation [$A = 0$ in Eq. (5)] are shown as the dashed lines in Fig. 2. In Fig. 2(a) the measured low-temperature rates fall significantly below this prediction, while in Fig. 2(b) the estimate is fairly accurate. The results are thus consistent with the effect of increased dissipation giving a smaller rate. Indeed, if we treat the numerical factor A in Eq. (5) as an adjustable parameter, excellent agreement of the data is found for $A \approx 4.5$. This tunneling rate, corrected for dissipation ($A = 4.5$), is shown as the dotted lines in Fig. 2.

An alternate method of displaying the data is presented in Fig. 3 which shows the width of the distribution $P(I)$, $\Delta I = \langle (I - \langle I \rangle)^2 \rangle^{1/2}$, vs T. As expected ΔI [which is proportional to the inverse slope of $\ln\tau^{-1}(I)$ vs I] becomes independent of T at low T. Also shown are the expected theoretical widths for thermal activation [Eq. (2)] and MQT tunneling with ($A = 4.5$) and without ($A = 0$) damping from Eqs. (3) and (5). It should be emphasized that there is little freedom in determining the junction parameters I_c, C, and R and that the only really adjustable parameter is the damping factor A (which has little effect on the low-I_c junction).

We believe that the measurements presented here are the first compelling evidence for the existence of quantum tunneling of a macroscopic variable. In fact, the low-I_c, high-β_c sample
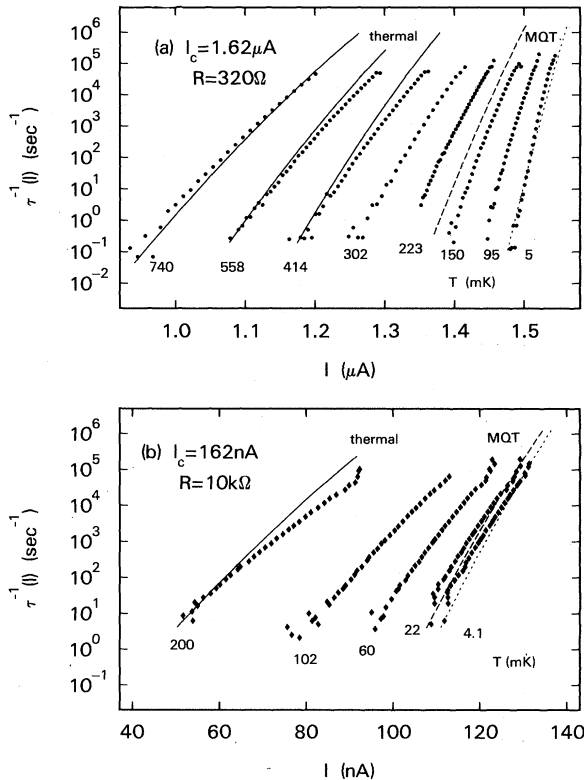

FIG. 2. Transition rates $\tau^{-1}(I)$ from the measured $P(I)$ for two junctions. (a) $I_c \approx 1.62$ μA, $R \approx 320$ Ω. (b) $I_c \approx 162$ nA, $R \approx 10$ kΩ. High-T theoretical thermal rates are shown as solid lines; MQT rates without damping are shown as dashed lines, with damping as dotted lines.
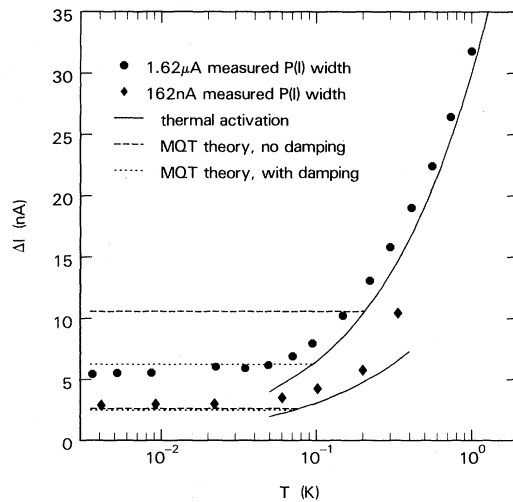

FIG. 3. Measured $P(I)$ widths $\Delta I = \langle (I - \langle I \rangle)^2 \rangle^{1/2}$ vs T for the two junctions. Theoretical predictions for thermal activation and MQT rates with and without damping are also shown.

shows a behavior close to the undamped predictions, while the higher-I_c sample demonstrates the reduction of tunneling rates due to dissipation. This reduction is consistent with the temperature-dependent rates found in high-current-density junctions.[9] The use of well characterized junctions [independent estimate of C and direct measurement of $R(T)$], the extension to very low temperatures, and the detailed measurement of $P(I)$ were important in being able to rule out extraneous effects and interpret the data within a theoretical framework. Although the observed reduction in tunneling rate ($A \approx 4.5$) is slightly greater than the expected $A \approx 1$, the magnitude is still reasonable. It is possible that the appropriate R in Eq. (5) is not the measured dc resistance near the origin (as used here) but either the high-frequency resistance or the quasiparticle resistance above the gap (in which case $A \approx 1.5$). Additional theoretical work is needed both on the effect of nonlinear and frequency-dependent damping and on the actual form of the crossover from thermal activation to macroscopic tunneling.

We acknowledge helpful discussions with A. J. Leggett, S. Kirkpatrick, and Y. Imry as well as the expertise of R. Laibowitz and S. Raider in preparing the all-Nb junctions.

[1]A. J. Leggett, J. Phys. (Paris), Colloq. 39, C6-1264 (1978).
[2]J. Kurkijarvi, in Proceedings of the Second International Conference on Superconducting Quantum Interference Devices and Third Workshop on Biomagnetism, Berlin, Germany, 6–9 May 1980, edited by W. de Gruyter (Physikalische–Technische Bundesanstait, Berlin, 1980), p. 247.
[3]A. O. Caldeira and A. J. Leggett, Phys. Rev. Lett. 46, 211 (1981); A. O. Caldeira, Ph.D thesis, University of Sussex, 1980 (unpublished).
[4]A. J. Leggett, in Proceedings of the Sixth International Conference on Noise in Physical Systems, Gaithersburg, Maryland, 1981 (to be published).
[5]A. Widom, G. Megaloudis, J. E. Sacco, and T. D. Clark, Nuovo Cimento 61B, 112 (1981).
[6]I. Affleck, Phys. Rev. Lett. 46, 388 (1981).
[7]W. den Boer and R. de Bruyn Ouboter, Physica (Utrecht) 98B+C, 185 (1980).
[8]R. J. Prance et al., Nature (London) 289, 543 (1981).
[9]E. L. Jackel et al., Bull. Am. Phys. Soc. 26, 382 (1981).
[10]T. A. Fulton and L. N. Dunkelberger, Phys. Rev. B 9, 4760 (1974).
[11]R. F. Voss, R. B. Laibowitz, S. I. Raider, and J. Clarke, J. Appl. Phys. 51, 2306 (1980).
[12]R. F. Voss et al., IEEE Trans. Magn. 17, 395 (1981).
[13]J. Magerlein, IEEE Trans. Magn. 17, 286 (1981).

Evidence for Elastic Disorder in the Elastically Ordered Phase of KCN

Harold T. Stokes

Department of Physics and Materials Research Laboratory, University of Illinois, Urbana, Illinois 61801

and

Thomas A. Case and David C. Ailion

Department of Physics, University of Utah, Salt Lake City, Utah 84112

We have obtained evidence from ^{13}C NMR measurements that the CN⁻ ion in the elastically ordered phase of KCN is misoriented slightly with respect to the orthorhombic b axis. This misorientation varies randomly over the lattice, averaging to zero on a macroscopic scale. The misorientations are manifested through small-angle CN⁻ reorientations which contribute to the spin-lattice relaxation time T_1 of the ^{13}C nuclei, via dipolar interactions and chemical shift anisotropy.

Potassium cyanide (KCN) exhibits an elastically ordered phase (below 168 °K) in which the CN⁻ molecules are aligned parallel to the b axis in an orthorhombic crystal structure[1,2] (see Fig. 1). In this phase, the CN⁻ molecules are disordered with respect to head-to-tail alignment and undergo random head-to-tail reorientations. The structure and dynamics of this system have been of considerable interest in recent years.[3-7]

We have studied this system by NMR of ^{13}C and from our results have been forced to conclude that, in the elastically ordered phase of KCN, small-angle reorientations as well as head-to-tail reorientations are taking place. This effect arises from the head-to-tail disorder of the CN⁻ molecules. Since the CN⁻ molecule is slightly different with respect to head and tail, this disorder breaks the orthorhombic symmetry of the